



Polyphosphoric acid–zirconia pillared clay composite catalytic system for efficient multicomponent one pot synthesis of tetrahydropyridines under environmentally benign conditions

Purabi Kar, B.G. Mishra *, S.R. Pradhan

Department of Chemistry, National Institute of Technology, Rourkela 769008, Odisha, India



ARTICLE INFO

Article history:

Received 8 January 2014

Received in revised form 22 February 2014

Accepted 24 February 2014

Available online 3 March 2014

Keywords:

Polyphosphoric acid

Zirconia pillared clay

Composite

Tetrahydropyridines

ABSTRACT

A series of zirconia pillared clay–polyphosphoric acid (PPA) composites are synthesized by adopting different preparative strategies. Initially, PPA is intercalated to the clay matrix with and without the use of structure expanding agent (CTAB). Subsequently, the PPA–clay composite is pillared with Zr-polycation to form the composite materials. In an alternate approach, Zr-pillared clay is synthesized by insertion of Zr-polycation, which is then used for dispersion of PPA moiety in the pillared clay matrix. The synthesized composites are characterized by XRD, FTIR, UV-vis, TGA, EDX, FE-SEM and sorptometric techniques. XRD study indicated an expansion in the clay structure after intercalation of PPA as well as the Zr-polycations. The FTIR spectra exhibit characteristic vibrational features of the clay sheet as well as PPA moiety indicating the structural stability of the composite materials. The phosphorous content in the composite samples is analyzed using EDX study. FE-SEM study indicated morphological changes upon intercalation of PPA and Zr-polycations to the clay matrix. The catalytic activity of the composite catalysts has been examined for the synthesis of tetrahydropyridines under environmental benign conditions by one pot multicomponent condensation of β -dicarbonyl compounds, substituted anilines and substituted benzaldehydes. The PPA intercalated clay pillared with Zr polycations (PPA-ZrP) is found to be highly efficient for the synthesis of structurally diverse substituted tetrahydropyridines under mild conditions.

© 2014 Elsevier B.V. All rights reserved.

1. Introduction

Clay materials are one of the most primordial and economic materials that have been used as adsorbents and as catalyst to carry out several acid catalyzed reactions. Although clays are used as catalysts, they possess certain disadvantages such as low thermal stability, loss of Brønsted acidic sites and collapsing of interlayer space at higher temperature [1,2]. To overcome these limitations, pillaring of clays with inorganic cationic nanoclusters has been done to enhance the thermal stability, pore volume, surface area and acidity of the clay. Pillared clays are a class of microporous materials with high surface area and acidic property. The intercalation of the inorganic cationic clusters imparts thermal stability generating new micropores and acidic sites in the clay materials. In the past years, these materials have been increasingly used as catalysts for several important catalytic reactions [3–6]. Pillared clays also provide a robust matrix for dispersion of catalytically

active components such as oxides, metals and organometallic complexes [3,7–10]. In recent years there have been efforts to exploit the acidic properties of pillared clay for synthesis of biologically important molecules under environmentally benign conditions. The Al-pillared clay has been found to be effective for the dispersion of the sulphated tin oxide (STO) nanoparticles. The STO/Al-P materials have been used as an efficient catalyst for synthesis of dihydropyrimidinones, coumarins and thiochromans. The synergism between the acidic sites of the pillared clay and the STO particles has been invoked to explain the higher catalytic activity observed for this material [3]. Similarly, chromia pillared clays have also been used as an efficient support to disperse silicotungstic acid (STA) nanoparticles. The STA/Cr-P materials show superior catalytic activity for the synthesis of dihydropyridines [11].

Polymeric acid display molecularly defined active sites suitable for a variety of chemical transformation. However, they possess inherent disadvantages such as low surface area and difficulty in separation and recovery when they are used in pristine form. In order to enhance their surface area, stability, and selectivity and to avoid corrosive property it is desirable to heterogenize these materials by dispersing in inorganic hard matrices by

* Corresponding author. Tel.: +91 0661 2462651; fax: +91 0661 2462659.

E-mail addresses: brajam@nitrk.ac.in, bmgcat@rediffmail.com (B.G. Mishra).

forming nanocomposites. In the present investigation, we have utilized the pillared clay as a host matrix to disperse polyphosphoric acid and studied their catalytic activity for synthesis of tetrahydropyridines. Polyphosphoric acid has promising application potential as catalyst in acid catalyzed organic transformations. Compared to other homogeneous corrosive acids, it is less corrosive, mild and exhibit dehydrating properties, which has been successfully exploited to carry out acylation and cyclization reaction of a variety of substrates [12–14]. PPA is also used as a catalyst for synthesis of heterocyclic compounds. The synthesis of 2-aryl/alkyl substituted benzimidazoles, benzoxazoles and benzothiazoles as well as purine derivatives has been accomplished by using PPA as catalyst [12,13]. Although there are reports on the catalytic activity of PPA, its applicability is limited due to disadvantages such as high viscosity and difficulty in separation and handling. In order to extend its effectiveness and to improve its recyclability, PPA has been supported over porous materials having high surface area such as SiO_2 [14]. The PPA- SiO_2 has been used as efficient catalyst for the multicomponent one pot synthesis of polyhydroquinoline derivatives, 1,8-octahydroxanthenes, N,N'-alkylidenebisamide derivatives and structurally diverse 3-benzoylisoxazoles [14–17]. Haniyeh Norouzi et al. have investigated the catalytic activity of the alumina supported PPA for the synthesis of 14-aryl-14H-dibenzo xanthenes [18]. Sachdev et al. have successfully synthesized SBA-15 supported PPA by direct as well as impregnation method and the efficiency of the prepared catalyst has been examined for the acylation of naphthalene in liquid phase using acetyl chloride as acylating agent [19].

Piperidine motifs are found in the basic skeleton of various natural alkaloids and pharmaceuticals [20]. Synthesis of various substituted piperidines has received considerable attention in recent years because of their antibacterial, anti-inflammatory, anticonvulsant and antimalarial properties [21]. Furthermore these moieties are highly active in inhibiting the action of cancer causing enzymes farneoyl transferase [22]. Hence different strategies are being developed for the synthesis of substituted tetrahydropyridines motifs. One pot multicomponent condensation reaction (MCR) is found to be most favourable way for the synthesis of these complex organic molecules within a very short period of time. MCR has certain advantages such as atom economy, shorter reaction time and eluding difficult purification processes. Earlier literature shows that lot of effort are being devoted by the researchers to develop a simple and easy protocol for the synthesis of substituted tetrahydropyridines by using various catalysts such as L-proline/TFA, bromodimethylsulfonium bromide (BDMS), tetrabutylammonium tribromide (TBATB), molecular iodine, ceric ammonium nitrate (CAN), $\text{ZrOCl}_2 \cdot 8\text{H}_2\text{O}$, picric acid and bismuth nitrate ($\text{Bi}(\text{NO}_3)_3 \cdot 5\text{H}_2\text{O}$) [22–29]. Although these catalysts have been found to be effective for the multicomponent condensation, they possess limitations in terms of greater reaction time, homogeneous nature of the reaction, requirement of higher amount of catalyst and cost ineffectiveness. To overcome such drawbacks we have employed PPA-Zr-pillared clay composite materials as catalyst for synthesis of various substituted tetrahydropyridines under environment benign conditions. In this study, different synthetic strategies are adopted to maximize the dispersion of the PPA in the clay and pillared clay matrix. The resulting composite materials are characterized by XRD, IR, FE-SEM, EDX, TGA, UV-vis and sorptometric techniques.

2. Materials and methods

The Na-montmorillonite ($\text{Na}_{0.35}\text{K}_{0.01}\text{Ca}_{0.02}$) ($\text{Si}_{3.89}\text{Al}_{0.11}$)^{tet} ($\text{Al}_{1.60}\text{Fe}_{0.08}\text{Mg}_{0.32}$)^{oct} $\text{O}_{10}(\text{OH})_2 \cdot n\text{H}_2\text{O}$ (Kunipia-F, Kunimine

industries, Japan) was used for the preparation of the pillared clay catalysts. The cation exchange capacity of the clay is 120 mequiv (100 g clay)⁻¹ which is determined using the method reported by Fraser and Russel [30]. Polyphosphoric acid (PPA) (85% P_2O_5), zirconium oxychloride ($\text{ZrOCl}_2 \cdot 8\text{H}_2\text{O}$), CTAB were procured from Loba Chemie Pvt. Ltd., India. Double distilled water prepared in the laboratory was used in the synthesis procedure.

2.1. Preparation of the catalyst

2.1.1. Preparation of PPA dispersed in parent clay matrix (PPA-clay)

2 g of clay material was dispersed in 50 mL of deionized water to form clay slurry. The slurry was sonicated for 15 min for better dispersion of the clay platelets. 0.4 mL of PPA was added to the clay suspension and the suspension was allowed to stir for 6 h. After stirring for the required amount of time, the excess water was removed by heating under vacuum. The resulting material was air dried and grinded to obtain the polycrystalline powder of PPA-clay.

2.1.2. Preparation of PPA intercalated clay using CTAB as a structure expansion agent (PPA-CTAB-clay)

5 g of montmorillonite clay was dispersed in 100 mL of double distilled water and stirred for 2 h at room temperature followed by sonication for 15 min to prepare clay slurry. 5 mmol of CTAB was completely dissolved in 50 mL of distilled water under 20 min of sonication. The CTAB solution was added dropwise to the clay slurry under continuous stirring at room temperature. The resulting suspension was stirred for 12 h. The ensuing solid material was filtered, washed three times with distilled water and then air dried at 110 °C overnight to obtain CTAB intercalated clay material. 2 g of CTAB-clay was subsequently dispersed in 50 mL of distilled water to which required amount of PPA (0.4 mL) was added. The resulting slurry was kept under continuous stirring for 12 h which was centrifuged, washed and dried overnight at 120 °C to obtain the CTAB-PPA-clay.

2.1.3. Preparation of PPA dispersed in Zr-pillared clay matrix (ZrP-PPA)

The 0.1 M Zr-pillaring solution was prepared by dissolving required amount of $\text{ZrOCl}_2 \cdot 8\text{H}_2\text{O}$ in 500 mL of water. The pillarating solution was subjected to heat treatment at 60 °C for 24 h. 5 g of clay was dispersed in 250 mL of water to form a clay suspension. To ensure well dispersion, the clay suspension was stirred at room temperature for 2 h followed by sonication for 15 min. The pillarating solution was added dropwise to the clay suspension at the rate of 50 mL/h under continuous stirring at room temperature. The mixture was stirred at room temperature for 24 h which was subsequently filtered and washed six times with deionised water to remove the chloride ions. The obtained gel was air dried at 120 °C followed by calcination at 500 °C for 2 h to obtain the Zr-pillared clay. 2 g of as synthesized zirconia pillared clay was dispersed in 50 mL of distilled water and was sonicated for 15 min. 0.4 mL of PPA was added to the Zr-P clay slurry under vigorous stirring. Stirring was continued for 6 h at room temperature. The solvent was evaporated by moderate heating under vacuum and the obtained solid particles were subsequently air dried at 120 °C to obtain the ZrP-PPA clay.

2.1.4. Preparation of PPA clay pillared with Zr-polycation (PPA-ZrP)

The Zr-pillaring solution was prepared as per the procedure described in Section 2.1.3. To a 2 g clay suspension in 50 mL water, 0.4 mL of PPA was added and stirred at room temperature for 6 h. 100 mL Zr-pillaring solution was added dropwise to the same pot at the rate of 50 mL/h under continuous stirring. The mixture was

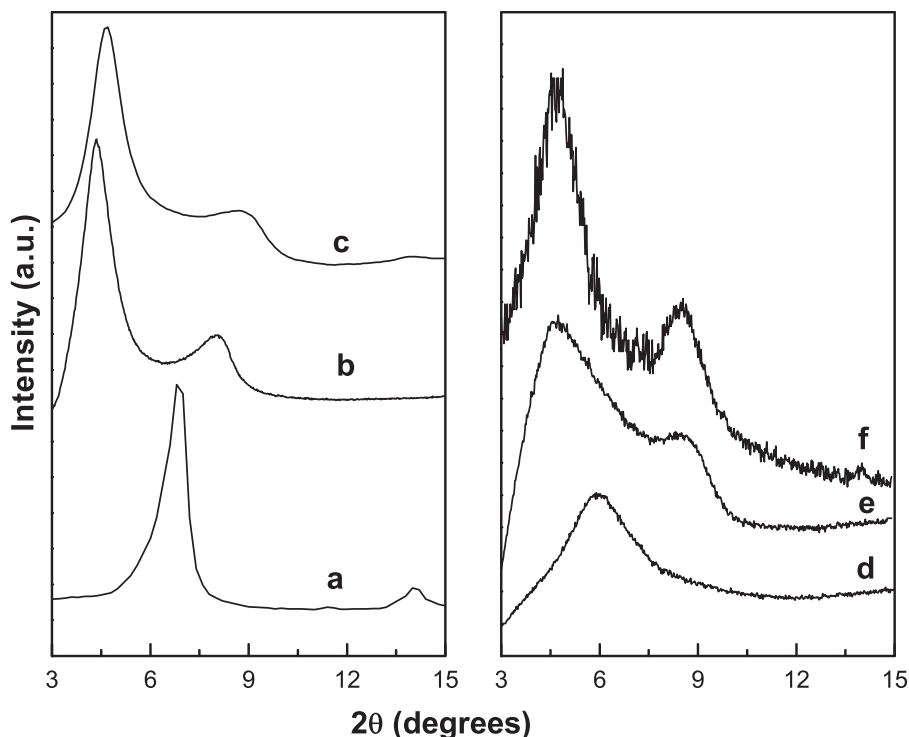


Fig. 1. XRD patterns of (a) parent clay, (b) air dried Zr-P, (c) calcined Zr-P, (d) PPA-clay, (e) PPA-ZrP and (f) ZrP-PPA.

then allowed for stirring at room temperature for another 12 h. The pillared clay particles were centrifuged and washed with deionized water. The resulting solid is air dried at 110 °C overnight, and heated at 300 °C for 2 h to obtain the PPA-ZrP clay material.

2.2. Characterization of the catalysts

The X-ray diffraction patterns of the clay material were recorded using a Rigaku Ultima-IV diffractometer using Ni filtered CuK α_1 ($\lambda = 1.5405 \text{ \AA}$) radiation. The XRD measurements were carried out in the 2θ range of 1–15° with a scan speed of 1 degree per minute using Bragg–Brantano configuration. The IR spectra of different clay samples (as KBr pellets) were obtained in transmittance mode by using Perkin-Elmer Infrared spectrometer with a resolution of 4 cm $^{-1}$ in the range of 400 cm $^{-1}$ to 4000 cm $^{-1}$. The UV-vis absorbance spectra of the sample were recorded using Shimadzu spectrometer model 2450 with BaSO₄ coated integration sphere in the range of 200–800 nm. Simultaneous thermogravimetric and differential scanning calorimetric analysis of the samples was performed on Netzsch, Model 449C apparatus in air atmosphere with linear heating rate (10 °C per min) from room temperature to 600 °C. The specific surface areas of the samples were determined by BET method using N₂ adsorption/desorption at 77 K on a Quantachrome Autosorb gas sorption system. The samples were degassed at 120 °C for 5 h prior to the sorptometric studies. Acidity of the prepared catalysts was determined by the nonaqueous titration method using the procedure reported elsewhere [4]. FESEM studies were performed by using Nova NanoSEM/FEI microscope. Prior to FESEM analysis the powder sample is placed on carbon tape followed by carbon coating. ¹H NMR spectra were recorded with Bruker 400 MHz NMR spectrometer using TMS as internal standard.

2.3. Catalytic activity study

The catalytic activity of the composite materials was evaluated for the synthesis of tetrahydropyridines. The synthesis of

Table 1
Basal spacing and surface area of different clay–PPA composite catalysts.

Material	Basal spacing (Å)	Surface area (m 2 /g)
Clay	12.8	30.2
Zr-P	19.0	176.0
PPA-clay	15.0	17.5
PPA-CTAB-clay	18.5	38.0
PPA-ZrP	19.2	95.2
ZrP-PPA	18.8	86.3

tetrahydropyridines was carried out by stirring a mixture of aryl aldehyde (2 mmol), ethylacetacetate (1 mmol), aniline (2 mmol) and 50 mg of different synthesized catalysts in acetonitrile solvent at 50 °C. The reaction was monitored by TLC. Catalytic activity was also examined at different temperatures and in different solvent media. After the completion of the reaction, the reaction mixture was filtered to separate the catalyst. The final product was recovered from the acetonitrile solution and recrystallized from ethanol to acquire the pure product. All the products obtained are known compounds and are characterized by comparing their physical and spectral characteristics with those reported in literature [22–29].

3. Results and discussions

3.1. Characterization of PPA-clay nanocomposite materials

The XRD patterns of the parent clay along with the Zr-pillared clay and clay–PPA composite materials in the 2θ range of 3–15° are presented in Fig. 1. The corresponding basal spacing values calculated from the XRD profile are presented in Table 1. The parent clay shows a sharp and intense peak at $2\theta = 6.8^\circ$ corresponding to the reflection from the {001} planes of the layered material. The basal spacing of the parent clay is calculated to be 12.8 Å (Fig. 1a). The intercalation of Zr-polyoxocationic clusters leads to the shifting of d_{001} peak to the lower 2θ value indicating an expansion in the clay structure due to pillaring (Fig. 1b). The as synthesized Zr-pillared

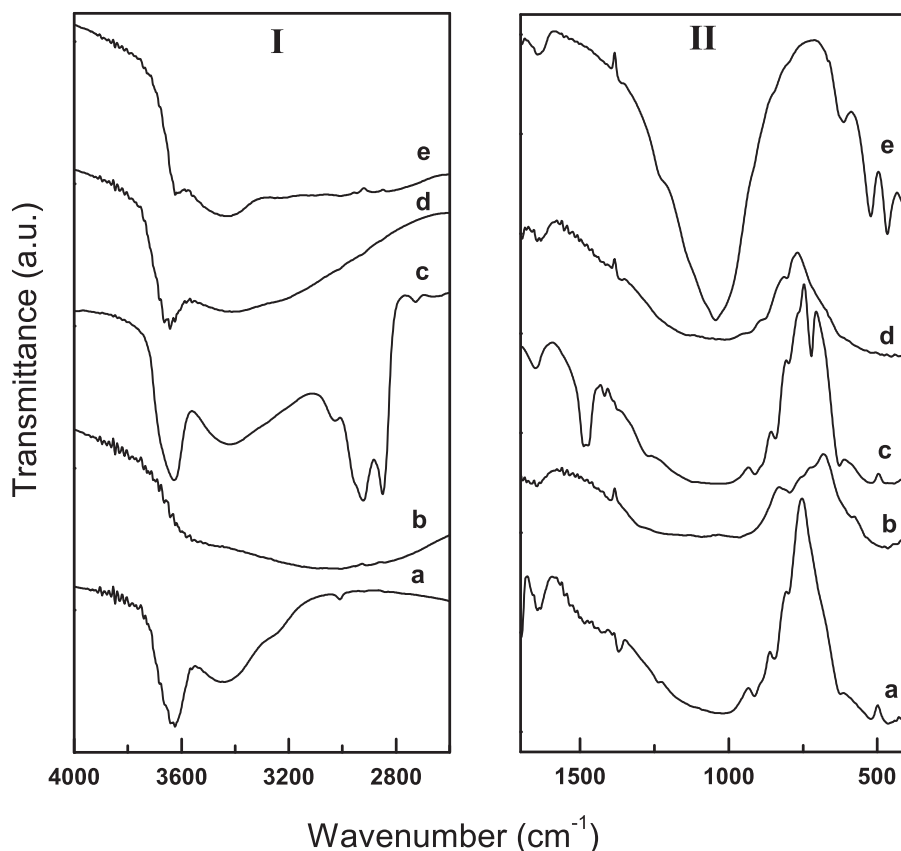


Fig. 2. FTIR spectra of (a) parent clay, (b) PPA-clay, (c) CTAB-PPA-clay, (d) ZrP-PPA and (e) PPA-ZrP (Panel I and Panel II in the range of 4000–3000 cm⁻¹ and 1700–400 cm⁻¹, respectively).

clay shows a basal spacing of 20.2 Å. On thermal treatment for 2 h at 500 °C, the Zr-pillared clay shows a slight shift in the peak position towards the higher 2θ value (Fig. 1c). This is due to conversion of the polyoxocations to oxide nanoclusters.

However, there is no appreciable difference in the intensity or broadness of the peak indicating the calcined Zr-pillared clay is stable up to 500 °C. The d_{001} value for the calcined Zr-P material is found to be 19.0 Å. From the XRD study it is illustrated that heat treatment up to 500 °C does not noticeably affect the crystallinity and stacking pattern of the pillared clay material. Fig. 1d–f shows the XRD patterns of different PPA-clay composite materials. Intercalation of PPA in general leads to the broadening of the peaks as compared to the respective clay materials. The broadening of the peak implies loss of crystallinity to a certain degree upon PPA intercalation. This may be attributed to mainly two factors. First, because of acidic nature of PPA, it can hydrolyze the Al–O–Si bond of the clay sheet which may result in disorder clay structure and consequent loss in crystallinity. However, considering the noncorrosive nature of PPA compared to other mineral acid this can occur to a small extent. The second important factor which can contribute to

the peak broadening is the formation of a well dispersed intercalated PPA-clay nanocomposite. Since PPA is intercalated to the clay matrix in swelled condition, it is likely that PPA molecules reside in the interlayer region. The presence of PPA molecules can disturb the stacking arrangement of the clay sheets along the [0 0 1] axis, which give rise to the disordered structure. The presence of PPA in the interlayer region is further evident from the shifting of peak towards lower 2θ value for the parent clay intercalated with PPA (PPA-clay). The d_{001} value observed for PPA-clay is 15 Å (Table 1).

The XRD pattern of the PPA-ZrP composite is shown in Fig. 1e. The XRD peak is broadened indicating a decrease in the crystalline character as compared to pure Zr-P. However, the noticeable point is that when the PPA-clay is crosslinked using Zr-polycation a basal spacing value (19.2 Å) similar to the Zr-pillared clay was obtained (Table 1 and Fig. 1e). This observation is indicative of the fact that the pillaring process imparts structural rigidity to the PPA-clay structure and the PPA molecules are trapped in the lateral space between the pillars. In case of ZrP-PPA materials, which is prepared by the dispersion of PPA molecules in the micropores of Zr-P, basal spacing value of 18.8 Å is observed (Fig. 1f).

Table 2
Physicochemical characteristics and catalytic activity of the clay-PPA composite materials.

Material	Acidic sites ^a (mmol g ⁻¹)	Phosphorous content (wt%)	Yield ^b (%)	Rate (mmol h ⁻¹ g ⁻¹)	Rate (mmol h ⁻¹ m ⁻² × 10 ⁻³)	TOF ^c (h ⁻¹)
PPA-clay	0.36	9.6	30.2	2.4	6.9	6.7
PPA-CTAB-clay	0.46	2.6	36.2	2.9	3.8	6.2
PPA-ZrP	0.73	7.1	83.3	6.7	3.5	9.1
ZrP-PPA	0.63	8.5	65.2	5.2	3.0	8.2

Reaction condition: benzaldehyde:aniline:ethylacetate 2:2:1, temperature 50 °C, 5 mL of acetonitrile, reaction time 5 h.

^a Calculated from non-aqueous titration.

^b Refers to pure and isolated yield.

^c Calculated with respect to the benzaldehyde conversion in the reaction mixture.

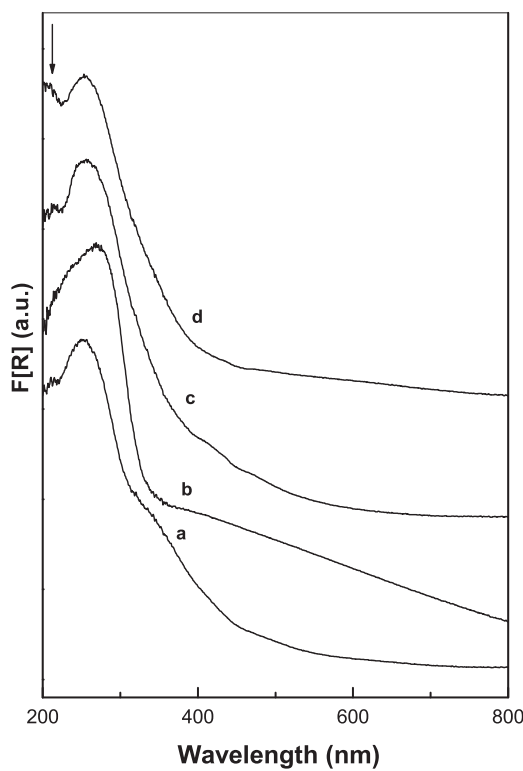


Fig. 3. UV-vis spectra of (a) parent clay, (b) PPA-clay, (c) ZrP-PPA and (d) PPA-ZrP.

The FTIR spectra of different clay materials are represented in Fig. 2. For parent clay, a sharp intense band is observed at 3636 cm^{-1} along with a broad less intense peak at 3450 cm^{-1} in the stretching frequency region of the FTIR spectrum (Fig. 2a, Panel I). These bands are assigned to the O–H stretching vibration from the structural

hydroxyl group and the water molecules present in the interlayer space of the clay materials, respectively [31]. Strained water molecules present in the first coordination sphere of the interlayer cations contribute significantly to the peak at 1636 cm^{-1} (Fig. 2a, Panel II) [29]. For the parent clay, three bands are observed at the finger print region at 915 , 845 and 805 cm^{-1} , which are attributed to the bending vibration modes of Al–Al–OH, Al–Mg–OH and Mg–Mg–OH groups, respectively, in the octahedral layer of the montmorillonite clay [31,32]. After the intercalation of the PPA to the clay, noticeable changes are observed in the stretching region of the FTIR spectra. The –OH stretching peak for PPA intercalated clay (Fig. 2b) is very broad that ranges from 3000 to 3600 cm^{-1} . The broadening of the –OH band can be ascribed to the formation of a variety of hydrogen bonding in presence of PPA inside the clay interlayer. The –OH group of PPA can form hydrogen bond with the –OH group of the clay sheet as well as the coordinated water molecule. Since the clay structure contain –OH groups differing in bond strength due to their location and coordination, it is expected that a wide range of hydrogen bonds of different strength can form in clay interlayer. These hydrogen bonds are responsible for broadening of the –OH peak [33]. PPA in its bulk state shows a prominent peak at 1015 cm^{-1} due to the stretching vibrations of P–O–P bond. The asymmetric stretching and bending vibration of P–O–P absorb IR radiation at 924 and 484 cm^{-1} , respectively [34]. These characteristic peaks with slight shift are observed for the clay–PPA composite materials which support the intercalation of PPA into the clay materials. For CTAB–PPA–clay, in addition to the characteristic peaks corresponding to the clay lattice and PPA, well distinguished peaks for CTAB are observed at 2851 and 2920 cm^{-1} after intercalation of PPA.

These peaks are ascribed to symmetric and asymmetric stretching vibrations of C–CH₂ present in the cetyl group of CTAB [35]. This observation implies the limited uptake of PPA in presence of CTAB. CTAB being an amphiphile generates a hydrophobic environment in the clay matrix which is not conducive for the intercalation

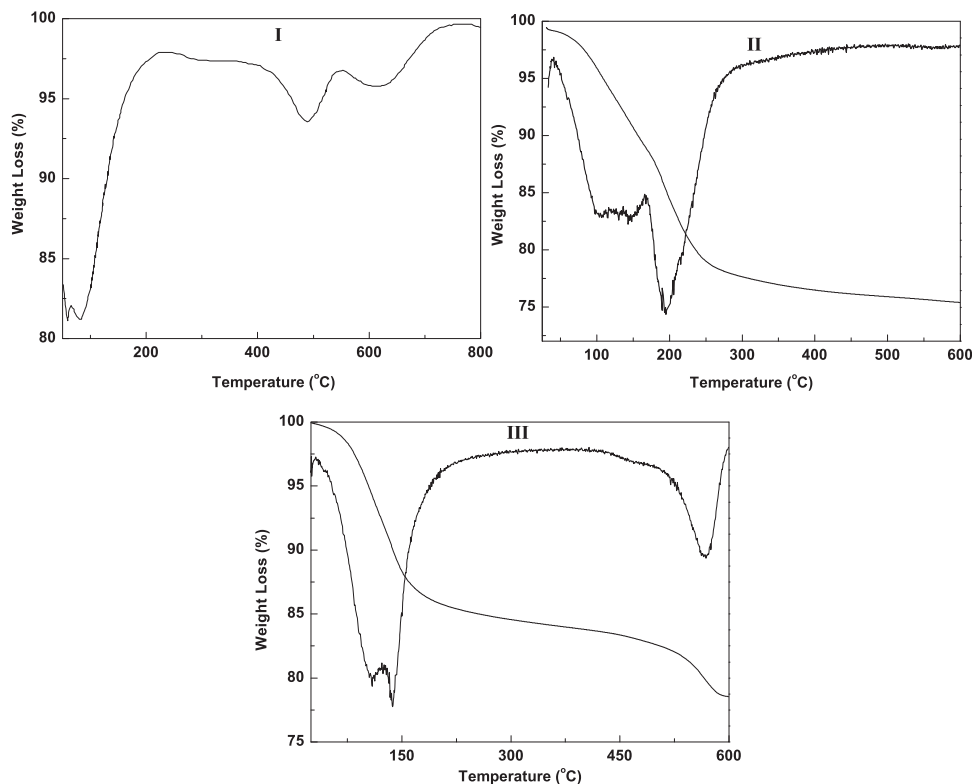


Fig. 4. Thermogravimetric profile of (I) Zr-P, (II) PPA-clay and (III) ZrP-PPA materials.

of PPA which is predominantly hydrophilic in nature. This fact is also evident from Table 2 which shows CTAB-PPA clay has less phosphorous content as compared to other clay materials.

The UV-vis spectra of the parent clay along with other clay polymer composite materials are presented in Fig. 3. The band observed at 247 nm (Fig. 3a) is characteristic for montmorillonite clay and attributed to the charge transfer transition for the structural iron present in the octahedral layer of the clay mineral ($\text{Fe}^{3+} \leftarrow \text{O}^{2-}, \text{OH}^-$ or OH_2) [4].

Upon incorporation of PPA into the clay matrix the band maxima was found to shift towards the higher wavelength side. The PPA-clay shows absorption maximum at 265 nm which is attributed to the change in coordination environment in the clay interlayer in presence of the PPA moieties. The same shift in band has also been observed for other composite materials. All the PPA containing composites shows the UV absorption maxima in the range of 255–265 nm. In case of the PPA-ZrP and ZrP-PPA an additional band is observed at 210 nm. This band can be ascribed to the Zr^{4+} (4d) $\leftarrow \text{O}^{2-}$ (2p) charge transfer transition from the zirconia nanopillars present in the clay interlayer [31].

The TGA profile of the air dried Zr-P, PPA-clay and ZrP-PPA clay materials is depicted in Fig. 4. Three major weight loss regions have been observed for the air dried Zr-pillared clay sample in the range of 50–200 °C, 400–550 °C and >550 °C (Fig. 4, Panel I). The removal of adsorbed water molecules present in the interlayer region of pillared materials is responsible for the weight loss between 50–200 °C. However, the weight loss detected in the range of 400–550 °C and >500 °C are accredited to the loss of structural water molecules and dehydroxylation of the pillars as well as clay sheets, respectively. The weight loss at high temperature region (>550 °C) is more gradual without any well-defined inflection point [4]. For ZrP-PPA three weight loss regions are also observed (Fig. 4, Panel III). The weight loss between 35–120 °C is due to the release of water molecules physically adsorbed into the pores of the clay matrix. The second weight loss between 125–180 °C is due to loss of water molecules coordinated to the pillars. These water molecules are in a coordinated state and hence require higher temperature for their removal. The third weight loss region observed in the temperature range 430–580 °C is ascribed to the removal of polyphosphoric acid. This weight loss is relatively sharp and can be clearly differentiated from the high temperature weight loss observed for air dried Zr-pillared clay sample.

The PPA-clay shows two major weight loss regions in the temperature range of 75–175 °C and 180–250 °C. The low temperature weight loss can be ascribed to the removal of physisorbed water molecules present in the clay interlayer and attached to the clay sheet. The weight loss in the region 180–250 °C is probably due to the removal of polyphosphoric acid in its monomeric form. Polyphosphoric acid is a linear polymer which contains mixture of oligomers of orthophosphoric acid up to 14 phosphorous units [36]. Polyphosphoric acid undergo hydrolysis at a very sluggish rate in presence of water to convert to its monomeric form i.e. orthophosphoric acid. The rate of hydrolysis becomes significant at higher temperature in presence of excess of water [37]. It is possible that the hydrophilic environment of the clay interlayer coupled with the constrained interlayer region of the clay can promote the hydrolysis of PPA to orthophosphoric acid (boiling point 160 °C) which is released in the temperature range of 180–250 °C. This hydrolysis process is suppressed to a greater extent in the Zr-pillared clay matrix. Although the hydrolysis of PPA in Zr-P matrix cannot be ruled out completely, a significant fraction of PPA remains in polymeric form and are removed in the temperature range of 430–580 °C which is the normal boiling point range of PPA used in this study.

The FE-SEM image of PPA-ZrP and ZrP-PPA composite materials is presented in Fig. 5. The PPA-ZrP composite material shows

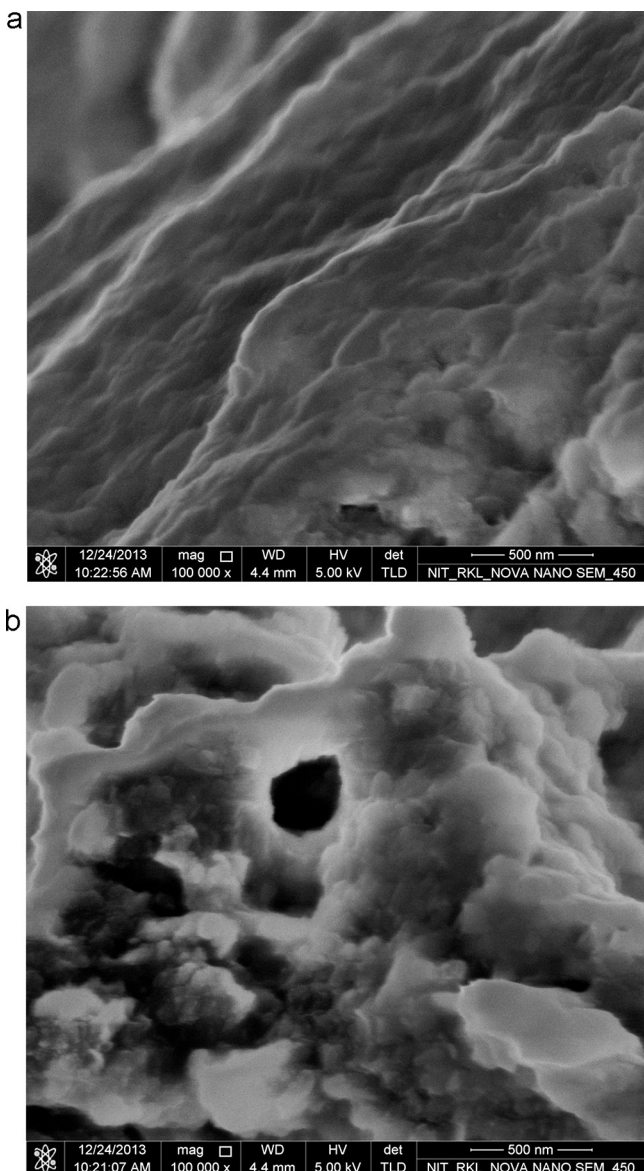
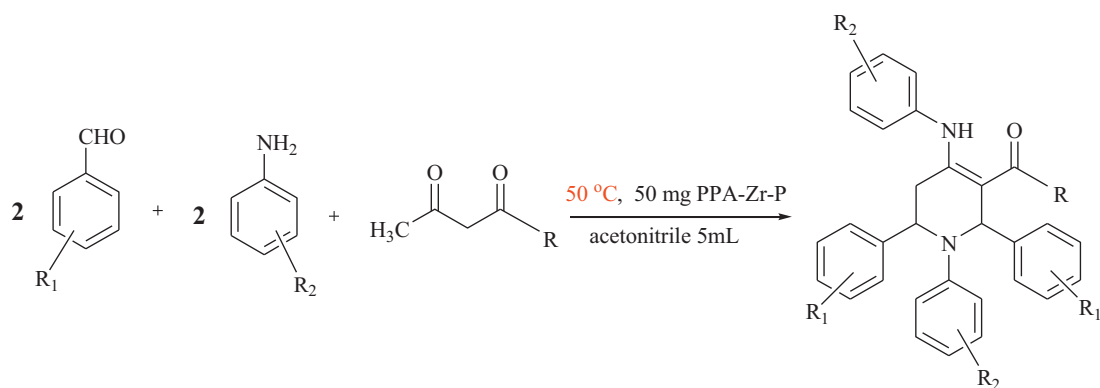


Fig. 5. FE-SEM images (a) PPA-ZrP and (b) ZrP-PPA.

relatively smooth surface extending up to the edge of the crystallites. The layer to layer orientation of the particles seems to be the favored orientation which leads to the morphology observed in Fig. 5a.

In case of the PPA-ZrP composite, the PPA molecules are present in the interlayer space which is sandwiched between the clay sheets. The protons present in the PPA molecules can form an electrical double layer between the clay sheets facilitating the face to face interaction. Where as in case of ZrP-PPA, the pillaring of the clay with the Zr-polycations provides structural rigidity to the clay lattice. Upon dispersion of the PPA in the Zr-P matrix, the PPA molecules occupy the micropores as well as the external surface. The presence of the PPA and its subsequent interaction with the faces and edges of the Zr-P crystallites distorts the lamellar structure of the clay platelets which results in particles with folded morphology (Fig. 5b). The surface area of the composite materials was determined by N_2 sorption. Pure clay shows Type-I adsorption isotherm according to the BDDT classification indicating the material to be microporous in nature (figure not shown). Pillaring with the Zr-pillared clay significantly increases the microporous character of the clay material. There is a significant increase in the



Scheme 1. Synthesis of tetrahydropyridines by multicomponent one pot condensation of arylaldehydes, substituted aniline and β -dicarbonyl compounds.

surface area and pore volume after pillaring with the Zr-polycation. The pillared clay-PPA composite shows lower value of surface area compared to the pure Zr-pillared clay due to the blockage of the micropores by the polymeric material.

3.2. Catalytic studies for synthesis of tetrahydropyridines

The catalytic activity of the clay-polymer composite systems is evaluated for the synthesis of tetrahydropyridines (THP) by one-pot multicomponent condensation of arylaldehydes, substituted aniline and β -dicarbonyl compounds at 50 °C using acetonitrile as solvent (Scheme 1).

At first emphasis is led on optimizing the reaction condition. Multicomponent reaction of benzaldehyde, aniline, and ethylacetacetate served as paradigm reaction for optimization. Initially, different clay-PPA composite materials synthesized in this work are evaluated for their activity using the model reaction. Table 2 shows the physicochemical characteristics of different clay-PPA

composite systems along with the yield of THP obtained after 5 h of reaction. Among all the composite materials the PPA-ZrP shows highest yield of the product. This material also exhibits higher surface area and acidic property compared to other composite materials. Since the composite materials display different physicochemical characteristics, the reaction rates are calculated in terms of unit surface area and per gram of the material which is presented in Table 2. It is observed that among all the composite catalyst, the PPA-ZrP shows higher reaction rate per gram of the material. The higher reaction rate per unit surface observed for the PPA-clay composite material is due to the higher density of phosphorous atom per unit area compared to other catalyst. This material contains higher percentage of phosphorous atom as observed from the EDAX analysis. However, in terms of total number of acidic site exposed to the surface, the PPA-clay display less number of sites compared to other catalyst. This is due to the fact that the PPA blocks the micropore of the clay material significantly decreasing its exposed surface. Moreover, due to the diffusional

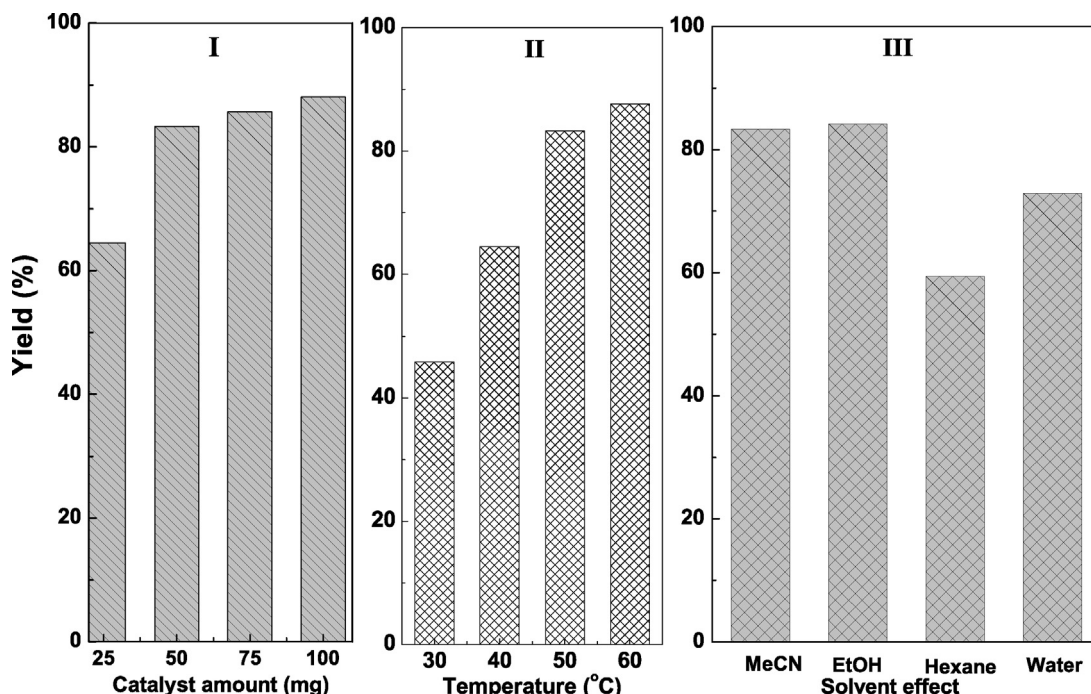


Fig. 6. Effect of catalyst amount, temperature and solvent on percentage yield of the tetrahydropyridine synthesized by one-pot multicomponent reaction of benzaldehyde, aniline and ethylacetacetate.

Table 3

Catalytic activity of PPA-ZrP composite materials for the synthesis of tetrahydropyridines by multicomponent condensation of arylaldehydes, substituted aniline and β -dicarbonyl compounds.

Sl no	R	R ₁	R ₂	Yield (%)
1	OCH ₃	4-NO ₂	H	68.1
2	OC ₂ H ₅	4-NO ₂	H	74.3
3	C ₆ H ₅	4-NO ₂	H	62.7
4	OCH ₃	4-Cl	H	75.3
5	OC ₂ H ₅	4-Cl	H	82.4
6	C ₆ H ₅	4-Cl	H	68.2
7	OCH ₃	4-F	H	81.2
8	OC ₂ H ₅	4-F	H	79.8
9	C ₆ H ₅	4-F	H	72.6
10	OCH ₃	H	H	78.5
11	OC ₂ H ₅	H	H	83.3
12	C ₆ H ₅	H	H	74.5
13	OCH ₃	4-OCH ₃	H	76.6
14	OC ₂ H ₅	4-OCH ₃	H	84.5
15	C ₆ H ₅	4-OCH ₃	H	68.4
16	OC ₂ H ₅	H	4-Cl	78.0
17	OC ₂ H ₅	H	2-Cl	72.0
18	OC ₂ H ₅	H	3-OH	90.4
19	OC ₂ H ₅	H	4-F	70.8
20	OC ₂ H ₅	H	4-OCH ₃	88.2
21	OC ₂ H ₅	H	4-NO ₂	66.7
22	OC ₂ H ₅	H	2-OH	86.2

constraint the internal sites remain inaccessible for catalysis. The turn over frequency (TOF) calculated for all the composite materials are presented in **Table 2**.

The PPA-ZrP shows highest TOF compared to other composite materials. The PPA-ZrP material has been selected for further study for THP synthesis. The amount of catalysts in the reaction mixture is varied between 25 mg and 100 mg. It is observed that for reaction involving 2 mmol of benzaldehyde, the yield of the reaction improves with catalyst amount up to 50 mg. Further increase in the catalyst amount only marginally influences the yield of the products (**Fig. 6**, Panel I).

Hence the catalyst amount was fixed at 50 mg. The effect of reaction temperature is studied by varying the temperature in the range of 30–60 °C. It is observed that with increase in temperature the THP yield increases significantly up to 50 °C. Further increase in temperature to 60 °C marginally improves the yield (**Fig. 6**, Panel II). Hence in this study, the reaction temperature is fixed at 50 °C. In order to study the effect of reaction media on the catalytic activity, solvents with different polarity are used in the optimized reaction protocol. It is noticed that for nonpolar solvent such as hexane the yield of the product is very less. The yield is found to improve upon use of polar solvent. Among different solvent tried for the reaction, comparable yields of the THP are obtained in acetonitrile and ethanol. Hence acetonitrile is used as a solvent for further study (**Fig. 6**, Panel III).

After optimizing the reaction conditions, we further investigated the scope and limitation of the optimized protocol using different β -dicarbonyl compounds, substituted aldehydes and substituted anilines (**Table 3**). It is observed that aniline substituted with electron donating groups is more active for the synthesis of THPs. The mechanistic pathway for formation of THP has been reported earlier [25]. The aniline reacts with one mole each of β -dicarbonyl compound and arylaldehyde to form the corresponding enamine and imine, respectively. Subsequently, the enamine undergoes intermolecular Mannich reaction with imine to generate an intermediate. This intermediate reacts with aldehyde followed by cyclization by intramolecular Mannich reaction to form the THPs. The presence of electron donating group in the substituted aniline increases the nucleophilicity of the amine group thereby facilitating the formation of enamine and imine. Upon variation of β -dicarbonyl compounds, it is noticed that the yield of the products are better in case of ethylacetacetate as compared

to that of methyl acetoacetate (**Table 3**). The minimum yield is observed when benzoyl acetone is used as β -dicarbonyl compound in the optimized protocol. The higher yield observed ethylacetacetate can be attributed to the greater acidic character of the alpha protons which facilitate the formation of the enamine. In case of benzoyl acetone the $-\text{COC}_6\text{H}_5$ group has electron withdrawing tendency and hence display weak acidic protons compared to its ester counterparts. However, for substituted aromatic aldehydes the electronic effect of the electron withdrawing or electron donating groups do not have much impact over the yield of the product. Among all aldehydes, the yield of the THP is less for p-nitrobenzaldehyde as compared to other substituted benzaldehydes. This is due to greater stability of the imine as the conjugation is extended to the $-\text{NO}_2$ group. After completion of the reaction, the catalyst particles are filtered from the reaction mixture. The catalyst is washed three times with 10 mL portion of ethanol and subsequently heat treated at 300 °C for 2 h to regenerate the catalyst. The recyclability of the catalyst is studied for three consecutive cycles without any significant loss in activity (**Table 3**, entry 11, yields, 83%, 1st; 80%, 2nd; 78%, 3rd).

4. Conclusions

In this work, we have reported the synthesis, characterization and catalytic application of novel polyphosphoric acid-zirconia pillared clay nanocomposite systems. The PPA molecules are intercalated into the clay lattice which is subsequently pillared with Zr-polycations to trap the PPA inside the clay interlayer. The expansion of the clay structure upon PPA intercalation and subsequent pillaring with Zr-polycation was confirmed from XRD study. The characteristic vibrational features of the clay and PPA moiety remain intact in the composite material. The clay material retains the PPA molecules inside the clay interlayer as determined from the EDX analysis. Various substituted THPs are synthesized in high yield and purity by one pot multicomponent condensation of aromatic aldehydes, substituted aniline, and β dicarbonyl compounds using PPA-ZrP materials as heterogeneous catalyst. The PPA-ZrP material is found to be highly efficient for the synthesis of structurally diverse tetrahydropyridines. The protocol developed using the PPA-ZrP composite catalyst was found to be advantageous in terms of simple experimentation, shorter time, high yield and purity of the products and recyclable catalyst.

Acknowledgement

PK would like to thank NIT, Rourkela for senior research fellowship.

Appendix A. Supplementary data

Supplementary data associated with this article can be found, in the online version, at <http://dx.doi.org/10.1016/j.molcata.2014.02.024>.

References

- [1] A. Gil, L.M. Gandia, M.A. Vicente, *Catal. Rev. Sci. Eng.* 42 (2000) 145–212.
- [2] A. Gil, S.A. Korili, M.A. Vicente, *Catal. Rev. Sci. Eng.* 50 (2008) 153–221.
- [3] M. Sowmiya, A. Sharma, S. Parsodkar, B.G. Mishra, A. Dubey, *Appl. Catal. A* 333 (2007) 272–280.
- [4] B.G. Mishra, G. Ranga Rao, *Micropor. Mesopor. Mater.* 70 (2004) 43–50.
- [5] J.R. Jones, J.H. Purnell, *Catal. Lett.* 28 (1994) 283.
- [6] F. Kooli, Y. Liu, S.F. Alshahateet, P. Siril, R. Brown, *Catal. Today* 131 (2008) 244.
- [7] L.M. Gandia, M.A. Vicente, A. Gil, *Appl. Catal. B* 38 (2002) 295–307.
- [8] C.B. Molina, L. Calvo, M.A. Gilarranz, J.A. Casas, J.J. Rodriguez, *Appl. Clay Sci.* 45 (2009) 206–212.
- [9] S. Barama, C. Dupeyrat-Batiot, M. Capron, E. Bordes-Richard, O. Bakhti-Mohammed, *Catal. Today* 141 (2009) 385–392.

- [10] V. Ramaswamy, M. Sivarama Krishnan, A.V. Ramaswamy, *J. Mol. Catal. A: Chem.* 181 (2002) 81–89.
- [11] P. Kar, B.G. Mishra, *Chem. Eng. J.* 223 (2013) 647–656.
- [12] P. Sadanandam, V. Jyothi, M.A. Chari, P. Das, K. Mukkanti, *Tetrahedron Lett.* 52 (2011) 5521–5524.
- [13] D.W. Hein, R.J. Alheim, J.J. Leavitt, *J. Am. Chem. Soc.* 79 (1957) 427–429.
- [14] K. Itoh, T. Aoyama, H. Satoh, Y. Fujii, H. Sakamaki, T. Takido, M. Kodomari, *Tetrahedron Lett.* 52 (2011) 6892–6895.
- [15] A. Khojastehnezhad, F. Moeinpour, A. Davoodnia, *Chin. Chem. Lett.* 22 (2011) 807–810.
- [16] S. Kantevari, R. Bantu, L. Nagaraju, *J. Mol. Catal. A: Chem.* 269 (2007) 53–57.
- [17] M.R.M. Shafiee, *J. Saudi Chem. Soc.* 15 (2011).
- [18] H. Norouzi, A. Davoodnia, M. Bakavoli, M. Zeinali-Dastmalbaf, N. Tavakoli-Hoseini, M. Ebrahimi, *Bull. Korean Chem. Soc.* 32 (2011) 2311–2315.
- [19] D. Sachdev, A. Dubey, *Catal. Commun.* 39 (2013) 39–43.
- [20] A.R. Mohite, P.R. Sultane, R.G. Bhat, *Tetrahedron Lett.* 53 (2012) 30–35.
- [21] G.-V. Ramin, S. Hajar, *C. R. Chim.* (2013).
- [22] G. Brahmachari, S. Das, *Tetrahedron Lett.* 53 (2012) 1479–1484.
- [23] M. Misra, S.K. Pandey, V.P. Pandey, J. Pandey, R. Tripathi, R.P. Tripathi, *Bioorg. Med. Chem.* 17 (2009) 625–633.
- [24] A.T. Khan, T. Parvin, L.H. Choudhury, *J. Org. Chem.* 73 (2008) 8398–8402.
- [25] A.T. Khan, M. Lal, M.M. Khan, *Tetrahedron Lett.* 51 (2010) 4419–4424.
- [26] A.T. Khan, M.M. Khan, K.K.R. Bannuru, *Tetrahedron* 66 (2010) 7762–7772.
- [27] H.-J. Wang, L.-P. Mo, Z.-H. Zhang, *ACS Comb. Sci.* 13 (2011) 181–185.
- [28] S. Mishra, R. Ghosh, *Tetrahedron Lett.* 52 (2011) 2857–2861.
- [29] C. Mukhopadhyay, S. Rana, R.J. Butcher, A.M. Schmiedekamp, *Tetrahedron Lett.* 52 (2011) 5835–5840.
- [30] A.R. Fraser, J.D. Russell, *Clay Miner.* 8 (1969) 229–230.
- [31] S. Samantaray, S.K. Sahoo, B.G. Mishra, *J. Porous Mater.* 18 (2011) 573–580.
- [32] S. Bodoardo, F. Figueras, E. Garrone, *J. Catal.* 147 (1994) 223–230.
- [33] Y. Chen, Q. Wang, *Polym. Degrad. Stab.* 91 (2006) 2003–2013.
- [34] F. Zhang, J. Yu, *Constr. Build. Mater.* 24 (2010) 410–418.
- [35] X. Ma, F. Xu, L. Chen, Z. Zhang, Y. Du, Y. Xie, *J. Cryst. Growth* 280 (2005) 118–125.
- [36] R.F. Jameson, *J. Chem. Soc. 2* (1959) 752–759.
- [37] V.A. Platonov, *Fibre Chem.* 32 (2000) 325–329.